Real-Time Spatial Estimates of Snow-Water Equivalent (SWE)

Sierra Nevada Mountains, California

January 26, 2021

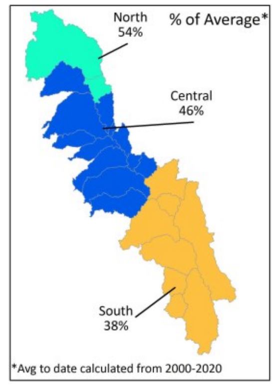

Team: Noah Molotch[1,2], Leanne Lestak[1], Keith Musselman[1], and Kehan Yang[1]
[1] Center for Water, Earth Science & Technology, Institute of Arctic and Alpine Research, University of Colorado Boulder
[2] Jet Propulsion Laboratory, California Institute of Technology
Contact: Leanne.Lestak@colorado.edu

Summary of current conditions

The regional summary map above shows the mean SWE above 5000' elevation for three major regions of the Sierra Nevada. As of January 26, regional average SWE remains below average across the Sierra, with percent of average SWE highest in the north (54%), central (46%) and lowest in the south (38%). While conditions are rapidly changing, this report summarizes snowpack conditions on January 26, before the onset of the latest and largest snow event impacting the region, though as of January 26th some snow has fallen and the snow line is down to 2000', snow depths are still relatively shallow. Detailed SWE maps (in JPG format) and summaries of SWE (in Excel format) by individual basin and elevation band accompany the report and are publicly available on our [FTP site](). Reports and tables are also available [here]().

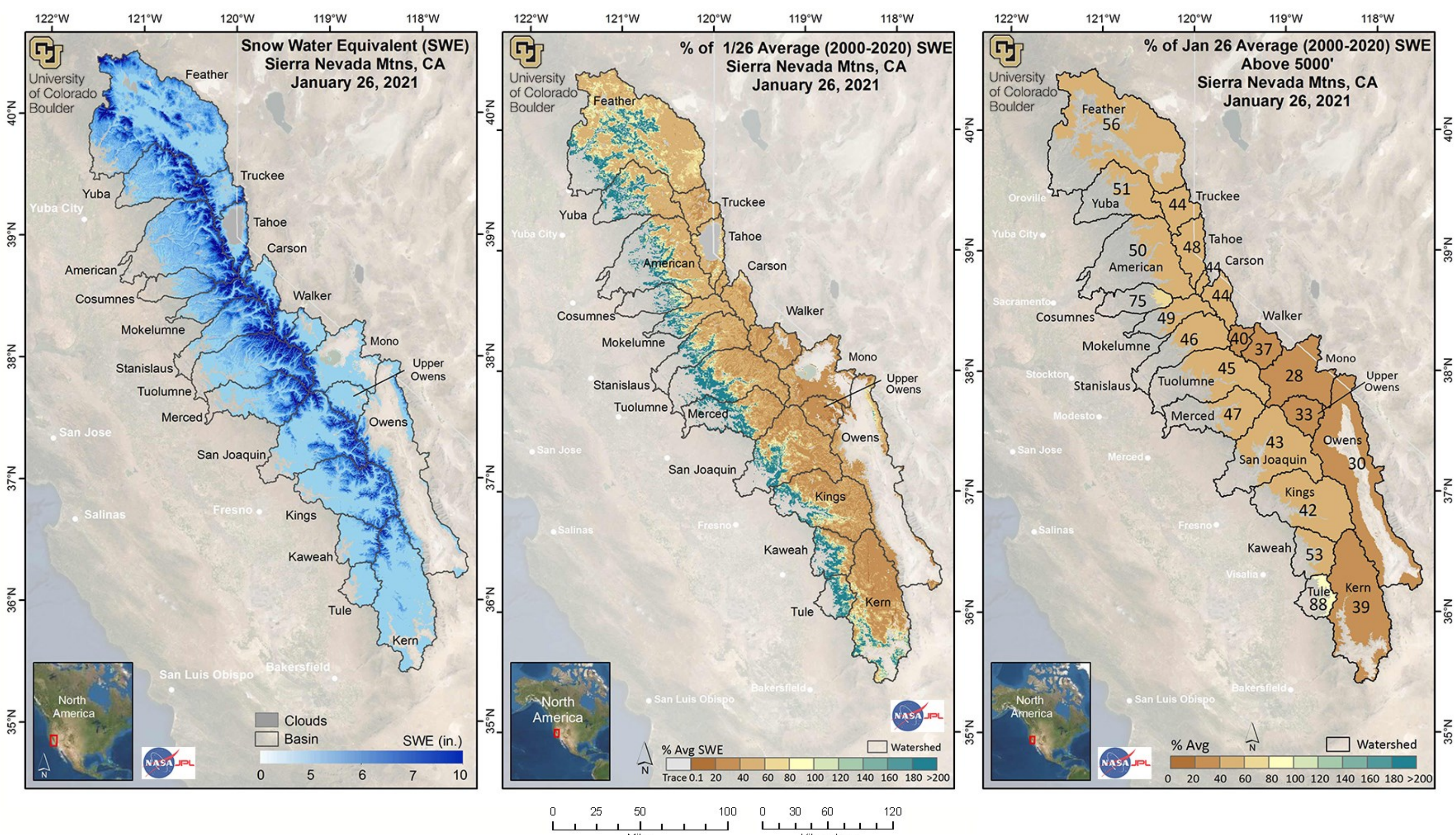

Figure 1. Estimated SWE and % of Average SWE across the Sierra Nevada. SWE amounts for January 26, 2021 (left), percent of average (2000-2020) SWE for January 26, 2021 for the Sierra Nevada, calculated for each pixel (middle) and basin-wide (right). Basin-wide percent of average is calculated across all model pixels >5000' elevation.

About this report

This is an experimental research product that provides near-real-time estimates of snow-water equivalent (SWE) at a spatial resolution of 500 m for the Sierra Nevada in California from mid-winter through the melt season. The report is released within a week of the date of data acquisition at the top of the report. A similar report covering the Intermountain West is available and is distributed to water managers in Colorado, Utah and Wyoming.

The spatial SWE analysis method for the Sierra Nevada uses the following data as inputs:

- In-situ SWE from all operational CA snow gage sensor sites and CoCoRaHS SWE values when available and applicable
- MODSCAG fractional snow-covered area (fSCA) data from recent cloud-free MODIS satellite images
- Physiographic information (elevation, latitude, upwind mountain barriers, slope, etc.)
- Historical daily SWE patterns (2000-2014) retrospectively generated using historical MODSCAG data and an energy-balance model that back-calculates SWE given the fSCA time-series and meltout date for each pixel

For more details on the estimation method see the *Methods* section below. Please be sure to read the *Data Issues / Caveats* section for a discussion of persistent challenges or flagged uncertainties of the SWE product.

Data availability for this report

101 snow gage sites in the Sierra Nevada network were recording SWE values out of a total of 114 sites, 13 were offline, 1 was recording zero SWE, and 36 CoCoRaHS (www.cocorahs.org) sites were used (shown in black, red, yellow and green, respectively, in Figure 4, left map).

The value of spatially explicit estimates of SWE

Snowmelt makes up the large majority (~60-85%) of the annual streamflow in the Sierra Nevada. The spatial distribution of snow-water equivalent (SWE) across the landscape is complex. While broad aspects of this spatial pattern (e.g., more SWE at higher elevations and on north-facing exposures) are fairly consistent, the details vary a lot from year to year, influencing the magnitude and timing of snowmelt-driven runoff.

SWE is operationally monitored at just over a hundred snow gage sensor sites spread across the Sierra Nevada, providing a critical first-order snapshot of conditions, and the basis for runoff forecasts from the CA DWR, NRCS, and NOAA. However, conditions at snow sensor sites (e.g., percent of normal SWE) may not be representative of conditions in the large areas between these point measurements, and at elevations above and below the range of the sensor sites. The spatial snow analysis creates a detailed picture of the spatial pattern of SWE using snow sensors, satellite, and other data, extending beyond the snow sensor sites to unmonitored areas.

Interpreting the spatial SWE estimates in the context of SNOTEL

The spatial product estimates SWE for every pixel where the MODSCAG product identifies snow-cover. Comparatively, snow sensor samples 8-20 points per basin within a narrower elevation range. Thus, the basin-wide percent of average from the spatial SWE estimates is not directly comparable with the snow sensor basin-wide percent of average. A better comparison might be made with the % of average in the elevation bands (Table 2) that contain snow sensor sites.

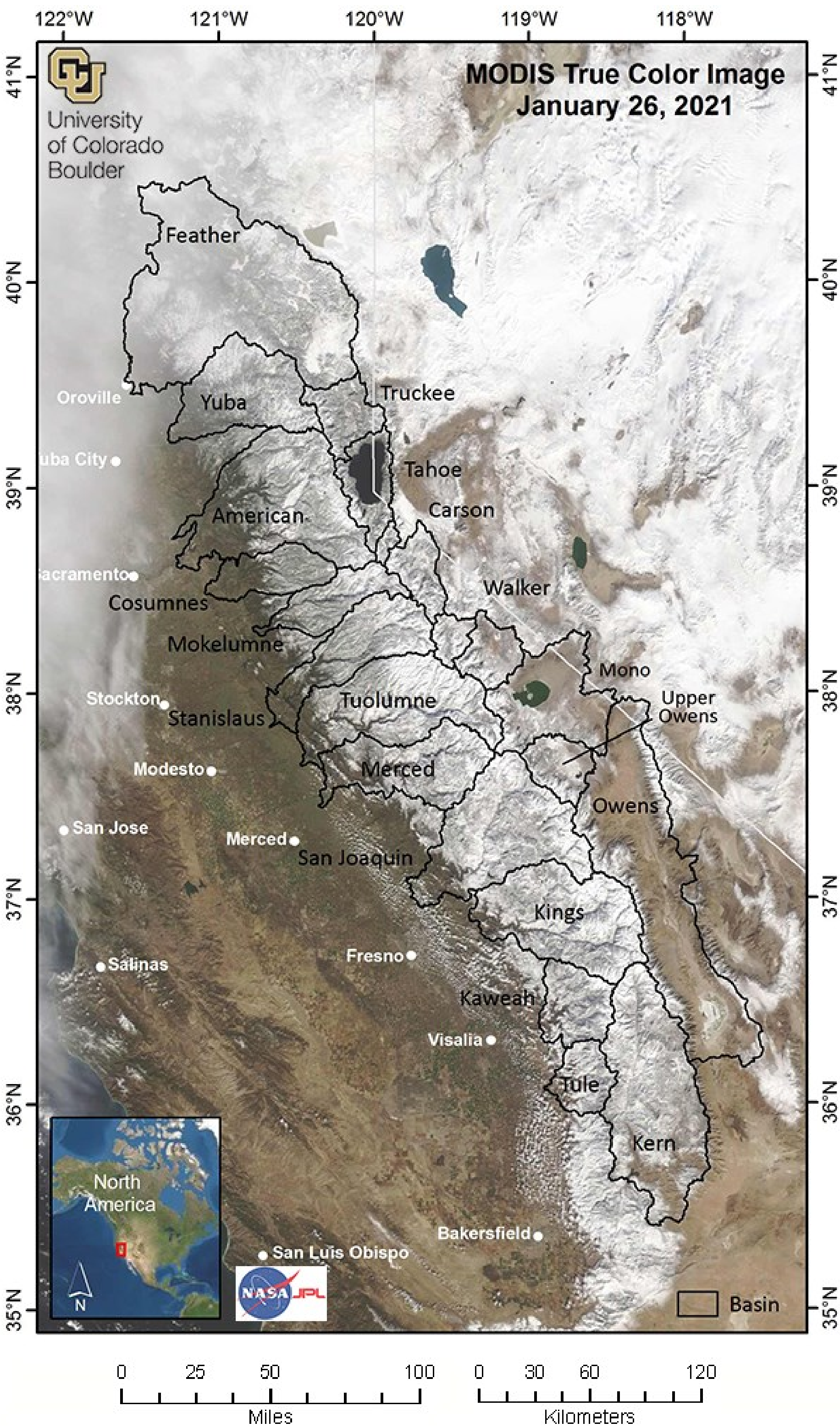

Figure 2. MODIS image, Sierra Nevada. A true color composite MODIS image, showing the sky view of the MODSCAG fractional snow-covered image used for the January 26, 2021 regression model run.

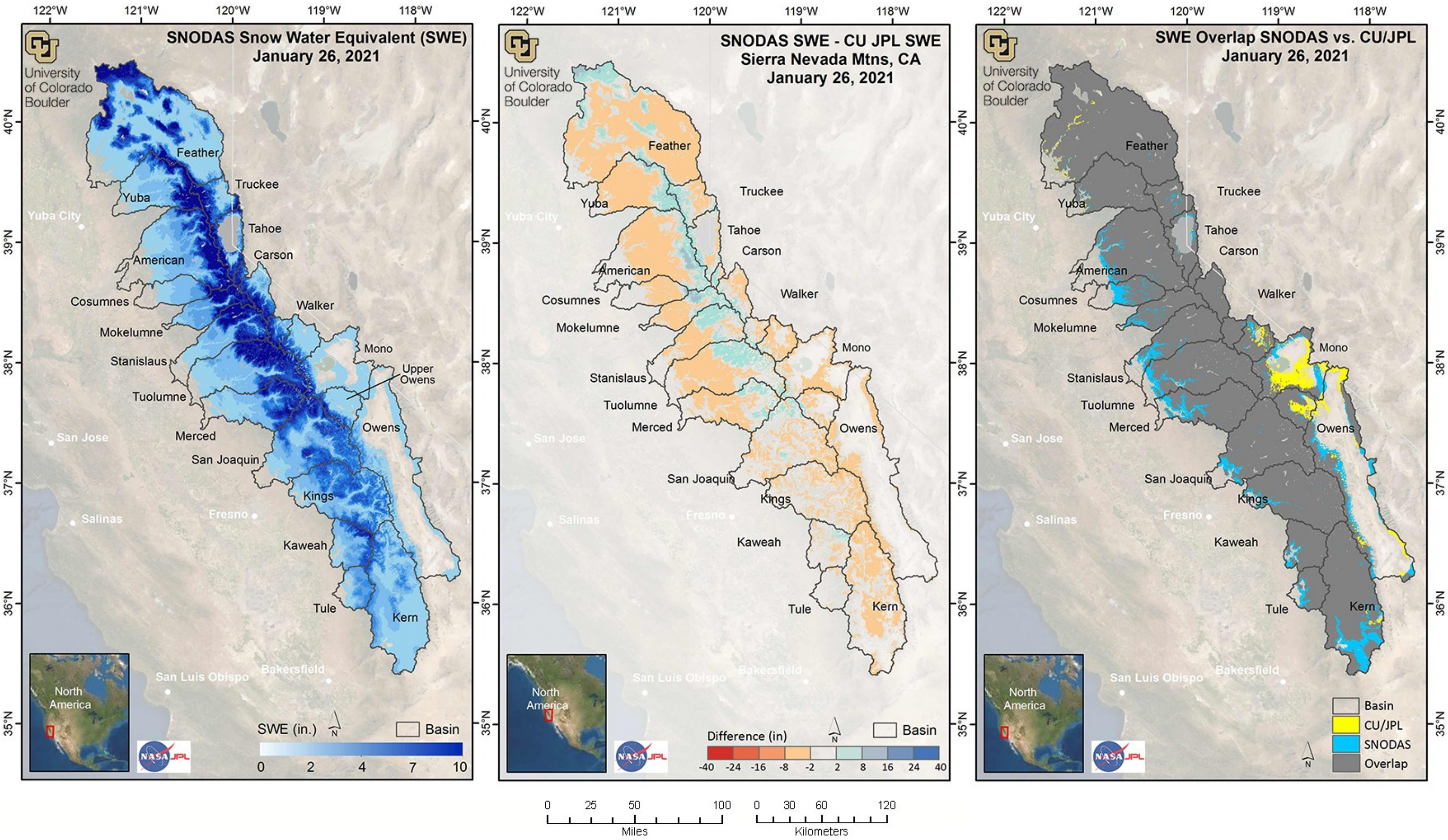

Figure 3. Comparison of CU/JPL regression SWE product and SNODAS SWE for the Sierra Nevada. The map on the left shows estimated SWE for January 26th from the NOAA National Weather Service's National Operational Hydrologic Remote Sensing Center (NOHRSC) SNOw Data Assimilation System (SNODAS). The middle map shows the difference between the January 26th SNODAS SWE estimate and CU/JPL regression SWE estimate. Red pixels denote areas where SNODAS SWE is less than CU/JPL SWE and blue pixels show areas where SNODAS SWE is higher than CU/JPL SWE. The map on the right shows the snow-cover extent of SNODAS and CU/JPL SWE estimates. Yellow pixels show where the location of CU/JPL snow extends beyond the location of the SNODAS snow extent. Blue pixels show where the SNODAS snow extends beyond the CU/JPL snow extent. Gray areas indicate regions where both products agree on the snow-cover extent.

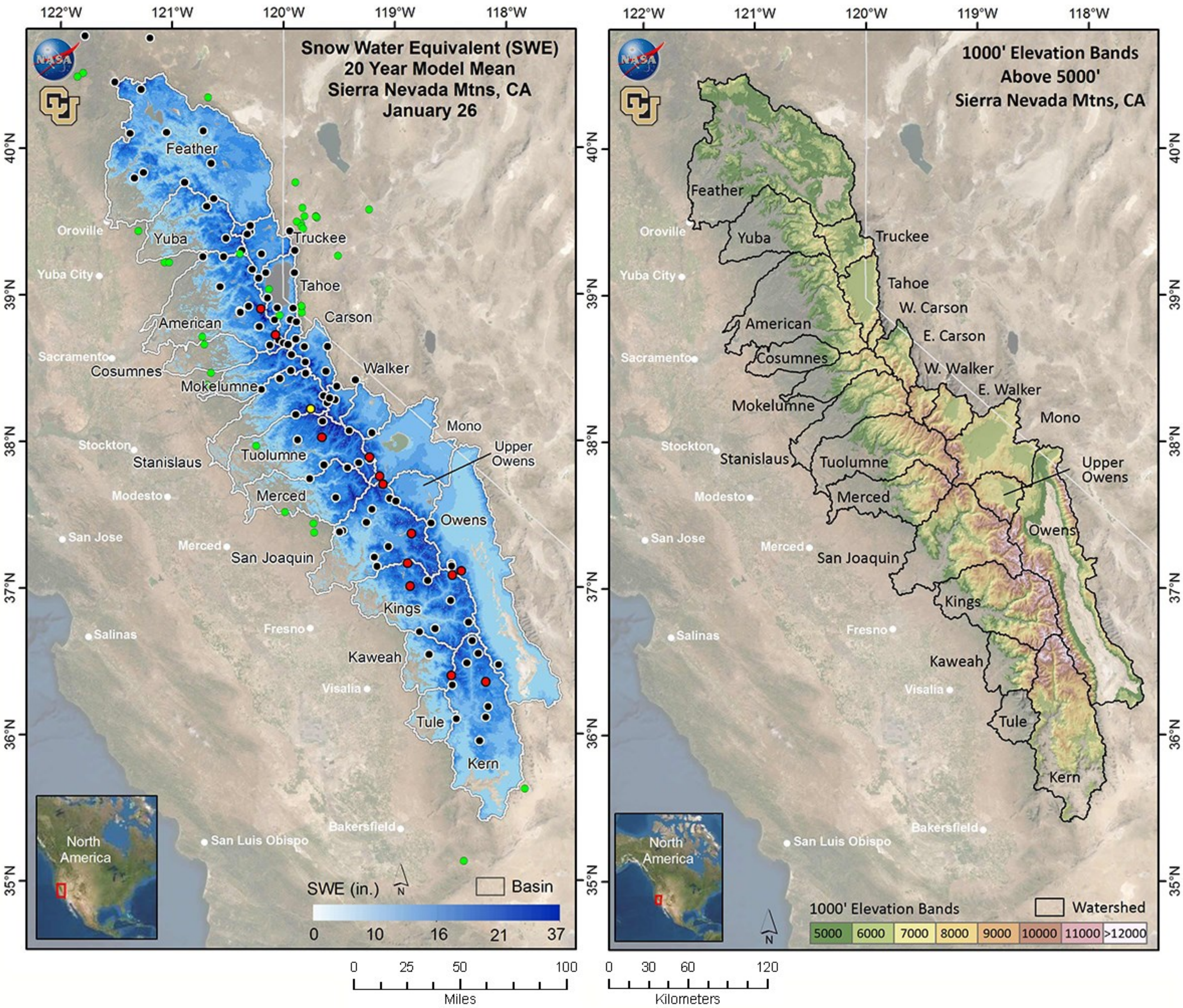

Figure 4. Historical average January 26th and Elevation Bands for the Sierra Nevada. Average SWE (2000-2020) for January 26th (left), and the Banded Elevation map (right) identifies basins used in this report (black boundaries) and 1000' elevation bands (colored shading) that match those used in Table 1 and Table 2. Map on left shows snow gage sensor sites recording SWE on January 26th (black), sites that were offline are shown in red, sites recording zero SWE are shown in yellow, and CoCoRaHS sites are shown in green.

Methods

The spatial SWE estimation method is described in Schneider and Molotch (2016). The method uses linear regression in which the dependent variable is derived from the operationally measured in situ SWE from all online snow sensor sites in the domain. The snow sensor SWE observations are scaled by the fractional snow-covered area (fSCA) across the 500 m pixel containing that snow sensor site before being used in the linear regression model. The fSCA is a combination of a near-real-time cloud-free MODIS satellite image which has been processed using the MODIS Snow Cover and Grain size (MODSCAG) fractional snow-covered area algorithm program (Painter, et. al. 2009, snow.jpl.nasa.gov) and the Snow Today fSCA image when necessary (Rittger, et. al. 2019, https://nsidc.org/snow-today).

The following independent variables (predictors) enter into the linear regression model:

- Physiographic variables that affect snow accumulation, melt, and redistribution, including elevation, latitude, upwind mountain barriers, slope, and others. See Figure 2 in Schneider and Molotch (2016) for the full set of these variables.
- The historical daily SWE pattern (1985-2016) retrospectively generated using historical MODSCAG data, and an energy-balance model that back-calculates SWE given the fractional Snow-Covered Area (fSCA) time series and meltout date for each pixel. See Margulis, et. al., 2016 for details. (For computational efficiency, only one image from either the 1st or 15th of

each month during the 1985-2016 period that best matches the real-time SNOTEL-observed pattern is selected as an independent variable.)

The real-time regression model for this date has been validated by cross-validation, whereby 10% of the SNOTEL data are randomly removed and the model prediction is compared to the measured value at the removed SNOTEL stations. This is repeated 30 times to obtain an average R-squared value, which denotes how closely the model fits the SNOTEL data. During development of this regression method, the model was also validated against independent historical SWE data collected in snow surveys at 9 locations in Colorado, and an intensive field survey in north-central Colorado.

Data Issues/Caveats for* January 26, 2021 *– IMPORTANT – READ THIS!

- DENSE FOREST COVER – Dense forest cover at lower elevations where snow-cover is discontinuous can cause the satellite to underestimate the snow-cover extent, leading to underestimation of SWE.
- CLOUD COVER – Cloud cover can obscure satellite measurements of snow-cover. While careful checks are made, occasionally the misclassification of clouds as snow or *vice versa* may result in the mischaracterization of SWE or bare-ground.
- RECENT SNOWFALL – There are occasionally problems with lower-elevation SWE estimates due to recent snowfall events that result in extensive snow-cover extending to valley locations where measurements are not available. This scenario results in an over-estimation of lower- elevation SWE.
- ANOMALOUS SNOW PATTERNS – Anomalous snow years or snow distributions may cause SWE error due to the model design to search for similar SWE distributions from previous years. If no close seasonal analogue exists, the model is forced to find the most similar year, which may result in error.

List of All Known Data Issues/Caveats

- RECENT SNOWFALL – There are occasionally problems with lower-elevation SWE estimates due to recent snowfall events that result in extensive snow-cover extending to valley locations where measurements are not available. This scenario results in an over-estimation of lower- elevation SWE.
- LIMITED SNOW PILLOW DATA – When snow at the snow pillow sites melts out, but remains at higher elevations, the model tends to underestimate SWE at the under-monitored upper elevations. This issue typically occurs late in the melt season, resulting in less accurate SWE prediction at higher elevations compared to earlier in the snow season.
- CLOUD COVER – Cloud cover can obscure satellite measurements of snow-cover. While careful checks are made, occasionally the misclassification of clouds as snow or *vice versa* may result in the mischaracterization of SWE or bare-ground.
- LOW LOOK ANGLE – When a satellite does not pass directly over a region but the area is still included within the satellite sensor's field of view, this is referred to as a low "look angle". The resulting image has lower effective resolution – this "blurry" MODSCAG data still contains useful information but may lead to overestimation of SWE near the margins of the snow-cover extent.
- POOR QUALITY SNOTEL DATA – Although data QA/QC is performed, occasional SNOTEL sensor malfunction may result in localized SWE errors.
- ANOMALOUS SNOW PATTERNS – Anomalous snow years or snow distributions may cause SWE error due to the model design to search for similar SWE distributions from previous years. If no close seasonal analogue exists, the model is forced to find the most similar year, which may result in error.
- DENSE FOREST COVER – Dense forest cover at lower elevations where snow-cover is discontinuous can cause the satellite to underestimate the snow-cover extent, leading to underestimation of SWE.

Table 1. Estimated SWE by basin. *The basin-wide SWE values and averages, are across all pixels at elevations >5000'. Shown are January 26th percent of January 26th average SWE (between 2000-2020 as derived from the regression model), January 26th mean SWE, January 26th percent of snow-covered area, January 26th water volume (acre-feet), the area (mi²) inside each basin that contains data pixels (not including cloud-covered pixels, lakes or other satellite no data pixels), January 26th snow pillow data, summarized for each basin. The last column shows January 26th mean SWE from SNODAS*.*

Basin	1/26/21 % 1/26 Avg.	1/26/21 SWE (in)	1/26/21 % SCA	1/26/21 Vol (af)	Area (mi2) > 5000'	1/26/21 Pillows	1/26/21 SNODAS* (in)
Feather	56	5.4	98.6	658,961	2,280.6	8.9 (7)	4.3
Yuba	51	6.5	98.6	193,017	556.9	15.8 (4)	6.8
American	50	6.2	98.3	282,116	852.1	8.8 (11)	6.8
Cosumnes	75	5.4	96.5	27,223	94.4	NA	4.5
Mokelumne	49	6.3	97.7	113,460	336.9	8.0 (1)	8.0
Stanislaus	46	5.9	97.9	186,136	591.9	7.2 (7)	6.5
Tuolumne	45	6.0	97.9	305,572	961.4	6.4 (7)	6.1
Merced	47	5.6	98.5	168,669	565.7	8.6 (2)	5.2
San Joaquin	43	5.1	97.4	343,219	1,274.1	3.1 (8)	3.7
Kings	42	4.9	96.0	331,940	1,261.1	4.5 (5)	2.9
Kaweah	53	4.4	95.5	77,120	325.7	0.7 (1)	3.6
Tule	88	3.8	100.0	28,871	143.2	2.9 (1)	2.5
Kern	39	3.3	94.5	305,454	1,749.6	2.7 (7)	1.2
Truckee	44	5.3	94.8	128,069	450.8	6.5 (4)	5.2
Tahoe	48	5.5	57.8	98,792	336.1	7.7 (8)	5.8
W Carson	44	6.0	98.9	22,619	70.6	7.7 (2)	6.6
E Carson	44	5.0	99.5	101,294	383.5	5.6 (5)	3.9
W Walker	40	5.6	97.7	57,435	192.1	6.1 (3)	4.6
E Walker	37	3.6	85.7	73,571	379.2	2.7 (1)	1.5
Mono	28	2.0	58.3	113,918	1,072.7	NA	0.7
Upper Owens	33	2.9	89.5	62,034	397.6	6.1 (1)	1.4
Owens	30	1.5	39.1	148,509	1,872.0	1.9 (4)	0.3

* This is a comparison to the SNODAS (SNOw Data Assimilation System) nationwide product from the National Weather Service.

Table 2. Estimated SWE by basin and elevation band. *Elevation bands begin at 5000' and extend past the highest point in the basin. Note that the area of the highest 2-5 bands is typically much smaller than the lower bands. Shown are January 26th percent of January 26th average SWE (between 2000-2020 as derived from the regression model), January 26th mean SWE, January 26th percent of snow-covered area, January 26th water volume (acre-feet), the area (mi²) inside each basin that contains data pixels (not including cloud-covered pixels, lakes or other satellite no data pixels), January 26th snow pillow data, summarized for each basin, summarized for each 1000' elevation band inside each basin. The last column shows January 26th mean SWE from SNODAS*.*

Basin	Elevation Band	1/26/21 % 1/26 Avg.	1/26/21 SWE (in)	1/26/21 % SCA	1/26/21 Vol (af)	1/26/21 Area (mi2)	1/26/21 Pillows	1/26/21 SNODAS* (in)
Feather	5000-6000'	59	4.9	98.0	357,072	1,358.5	3.7 (1)	3.0
	6000-7000'	53	6.0	99.5	250,953	790.4	9.6 (5)	5.8
	7000-8000'	49	7.2	99.6	48,899	127.1	10.3 (1)	9.1
	8000-9000'	41	8.3	100.0	2,037	4.6	NA	9.0
Yuba	5000-6000'	57	5.4	98.6	59,323	204.2	NA	2.4
	6000-7000'	49	6.6	98.2	80,893	230.1	14.9 (3)	7.9
	7000-8000'	48	8.0	99.5	50,651	118.1	18.6 (1)	12.1
	8000-9000'	42	9.0	100.0	2,150	4.5	NA	14.7
American	5000-6000'	58	5.1	98.2	85,418	314.0	4.3 (3)	2.4
	6000-7000'	48	6.0	98.6	90,291	281.5	12.2 (2)	6.8
	7000-8000'	49	7.3	98.4	68,950	176.8	10.2 (4)	12.3
	8000-9000'	45	8.6	97.5	32,553	70.6	9.5 (2)	12.0
	9000-10,000'	44	10.1	99.2	4,904	9.1	NA	10.6
Cosumnes	5000-6000'	95	4.9	95.2	16,467	62.5	NA	2.1
	6000-7000'	59	6.1	98.6	8,053	24.9	NA	7.0
	7000-8000'	51	7.3	100.0	2,703	7.0	NA	16.0
Mokelumne	5000-6000'	66	4.8	93.5	22,536	88.6	NA	2.1
	6000-7000'	50	5.6	99.6	20,348	68.5	NA	7.6
	7000-8000'	48	6.8	99.5	33,163	91.0	NA	12.0
	8000-9000'	44	7.8	98.6	33,531	80.1	8.0 (1)	10.0
	9000-10,000'	41	8.4	100.0	3,883	8.6	NA	9.6
Stanislaus	5000-6000'	67	4.5	96.4	26,781	112.5	NA	1.7
	6000-7000'	46	5.0	96.7	37,922	141.4	6.1 (1)	6.4
	7000-8000'	44	5.9	98.5	47,968	152.2	10.4 (2)	8.6
	8000-9000'	42	7.0	99.6	44,215	118.5	6.3 (3)	8.1
	9000-10,000'	40	8.0	99.0	22,968	53.8	4.5 (1)	8.2
	10,000-11,000'	39	8.7	97.4	6,124	13.3	NA	5.6
	> 11,000'	39	8.5	100.0	158	0.3	NA	2.0
Tuolumne	5000-6000'	75	4.4	97.1	42,035	179.4	NA	1.4
	6000-7000'	48	4.8	98.5	37,788	147.2	2.2 (1)	3.8
	7000-8000'	43	5.6	98.3	46,942	157.6	6.6 (1)	7.7
	8000-9000'	42	6.4	98.4	58,717	173.2	6.8 (3)	8.2
	9000-10,000'	40	7.2	98.9	70,254	183.6	7.7 (2)	8.8
	10,000-11,000'	40	7.7	96.9	37,574	91.4	NA	7.6
	11,000-12,000'	41	7.9	90.6	10,957	26.0	NA	4.2
	> 12,000'	42	8.4	97.6	1,305	2.9	NA	2.1
Merced	5000-6000'	155	4.3	97.4	17,185	75.2	NA	1.3
	6000-7000'	61	4.5	97.6	20,026	82.9	NA	2.2
	7000-8000'	45	5.1	99.2	38,600	142.0	NA	4.8
	8000-9000'	43	5.9	98.6	38,960	124.5	8.6 (2)	7.3
	9000-10,000'	40	6.7	99.2	31,472	88.3	NA	8.4
	10,000-11,000'	39	7.8	98.1	16,435	39.7	NA	7.0
	11,000-12,000'	40	8.5	98.2	5,221	11.6	NA	4.7
	> 12,000'	40	9.0	100.0	769	1.6	NA	3.1

Basin	Elevation Band	1/26/21 % 1/26 Avg.	1/26/21 SWE (in)	1/26/21 % SCA	1/26/21 Vol (af)	1/26/21 Area (mi2)	1/26/21 Pillows	1/26/21 SNODAS* (in)
San Joaquin	5000-6000'	91	3.2	96.9	24,699	145.0	NA	1.2
	6000-7000'	46	3.5	97.9	34,791	186.8	3.5 (3)	2.0
	7000-8000'	43	4.0	97.8	47,948	222.5	2.6 (4)	3.1
	8000-9000'	42	5.0	99.2	54,324	203.4	NA	4.8
	9000-10,000'	39	5.9	98.3	65,233	207.3	4.0 (1)	5.9
	10,000-11,000'	39	6.8	97.2	58,143	161.4	NA	5.1
	11,000-12,000'	39	7.3	92.6	46,547	119.4	NA	3.6
	> 12,000'	39	7.6	92.9	11,533	28.5	NA	2.3
Kings	5000-6000'	105	3.1	98.0	16,595	101.5	NA	1.2
	6000-7000'	57	3.4	97.3	24,681	137.0	NA	1.6
	7000-8000'	43	3.9	98.9	36,417	177.3	4.1 (1)	2.5
	8000-9000'	42	4.7	97.7	54,889	221.3	NA	3.4
	9000-10,000'	39	5.4	98.1	63,402	221.8	6.5 (1)	4.2
	10,000-11,000'	38	6.0	96.0	62,129	194.0	4.0 (3)	3.9
	11,000-12,000'	39	6.6	88.3	54,818	155.1	NA	2.2
	> 12,000'	38	6.7	87.1	19,010	53.1	NA	1.0
Kaweah	5000-6000'	196	3.2	96.1	10,600	61.5	NA	1.6
	6000-7000'	91	3.5	95.8	11,442	60.7	0.7 (1)	1.9
	7000-8000'	53	4.1	96.4	13,654	62.4	NA	3.3
	8000-9000'	46	4.9	98.8	15,188	57.9	NA	4.8
	9000-10,000'	41	5.6	95.2	12,992	43.7	NA	6.1
	10,000-11,000'	37	6.2	88.6	10,298	30.9	NA	6.0
	11,000-12,000'	36	6.4	85.5	2,903	8.4	NA	4.1
	> 12,000'	33	5.7	100.0	42	0.1	NA	4.1
Tule	5000-6000'	232	3.3	100.0	9,635	55.2	NA	2.4
	6000-7000'	119	3.7	100.0	8,173	41.8	NA	2.3
	7000-8000'	59	4.2	100.0	6,002	26.8	2.9 (1)	2.4
	8000-9000'	46	4.8	100.0	3,819	14.8	NA	3.1
	9000-10,000'	38	5.1	100.0	1,200	4.4	NA	3.9
	10,000-11,000'	39	5.6	100.0	42	0.1	NA	3.4
Kern	5000-6000'	73	1.8	86.0	25,230	258.2	NA	0.7
	6000-7000'	52	2.3	92.6	44,706	358.5	NA	0.8
	7000-8000'	40	3.0	96.3	54,485	340.5	0.8 (1)	0.8
	8000-9000'	35	3.5	99.3	60,894	326.0	5.0 (2)	1.4
	9000-10,000'	34	4.0	99.2	41,507	193.5	2.9 (1)	1.9
	10,000-11,000'	34	4.9	96.7	34,664	133.4	2.2 (2)	2.3
	11,000-12,000'	35	5.7	90.3	28,957	94.8	1.0 (1)	1.5
	> 12,000'	36	6.3	90.1	15,010	44.6	NA	0.6
Truckee	5000-6000'	35	3.4	78.9	12,582	69.7	NA	0.8
	6000-7000'	44	4.7	96.8	55,727	221.7	6.5 (4)	4.1
	7000-8000'	48	6.7	99.7	43,018	120.0	NA	8.1
	8000-9000'	45	8.0	100.0	13,144	31.0	NA	10.2
	9000-10,000'	42	8.1	100.0	3,418	8.0	NA	9.2
	10,000-11,000'	38	8.0	100.0	180	0.4	NA	8.1

Basin	Elevation Band	1/26/21 % 1/26 Avg.	1/26/21 SWE (in)	1/26/21 % SCA	1/26/21 Vol (af)	1/26/21 Area (mi2)	1/26/21 Pillows	1/26/21 SNODAS* (in)
Tahoe	6000-7000'	45	3.6	33.5	25,561	131.5	6.5 (3)	2.9
	7000-8000'	52	6.0	97.1	35,993	113.4	8.5 (4)	7.0
	8000-9000'	48	7.5	98.9	29,277	73.1	8.2 (1)	8.5
	9000-10,000'	43	8.2	99.2	7,607	17.4	NA	9.1
	10,000-11,000'	39	7.9	100.0	355	0.8	NA	6.9
W. Carson	5000-6000'	65	3.0	100.0	33	0.2	NA	0.7
	6000-7000'	56	4.2	100.0	501	2.2	NA	2.0
	7000-8000'	43	5.1	99.8	8,780	32.3	NA	7.6
	8000-9000'	44	6.7	99.5	9,974	27.9	7.7 (2)	6.0
	9000-10,000'	43	7.9	95.2	3,040	7.3	NA	6.4
	10,000-11,000'	38	7.1	72.7	290	0.8	NA	6.5
E. Carson	5000-6000'	52	2.5	99.0	6,724	50.5	NA	0.7
	6000-7000'	43	3.4	98.9	14,047	78.5	1.8 (1)	1.1
	7000-8000'	43	4.7	99.5	26,064	104.9	5.3 (1)	3.6
	8000-9000'	44	6.2	100.0	34,033	102.1	6.9 (3)	6.1
	9000-10,000'	44	7.9	99.2	15,361	36.5	NA	8.0
	10,000-11,000'	42	8.6	100.0	4,952	10.7	NA	7.1
	> 11,000'	36	7.7	100.0	114	0.3	NA	5.0
W. Walker	6000-7000'	33	2.6	98.2	1,096	7.8	NA	0.9
	7000-8000'	34	3.1	93.9	6,758	41.1	2.3 (1)	1.6
	8000-9000'	40	4.8	98.8	12,319	48.3	4.7 (1)	3.9
	9000-10,000'	41	7.0	98.6	24,385	65.3	11.2 (1)	7.0
	10,000-11,000'	41	8.2	99.0	11,973	27.3	NA	5.6
	> 11,000'	39	7.6	100.0	904	2.2	NA	3.5
E. Walker	6000-7000'	19	1.1	57.1	3,541	60.7	NA	0.1
	7000-8000'	32	2.3	85.1	14,984	120.5	NA	0.4
	8000-9000'	40	3.8	95.2	19,627	96.5	NA	1.3
	9000-10,000'	43	5.9	96.8	18,076	57.7	2.7 (1)	3.9
	10,000-11,000'	43	7.4	94.9	13,740	34.9	NA	4.0
	11,000-12,000'	43	7.6	92.8	3,514	8.7	NA	2.3
	> 12,000'	44	7.8	100.0	87	0.2	NA	1.4
Mono	6000-7000'	7	0.3	18.0	4,772	322.0	NA	0.0
	7000-8000'	24	1.5	69.0	33,397	419.5	NA	0.1
	8000-9000'	35	3.0	92.0	29,523	186.8	NA	0.6
	9000-10,000'	40	4.7	95.6	16,362	65.2	NA	3.1
	10,000-11,000'	41	6.6	93.3	17,269	48.7	NA	6.0
	11,000-12,000'	44	7.8	93.9	10,782	26.1	NA	3.9
	> 12,000'	42	7.7	96.8	1,813	4.4	NA	2.0
Upper Owens	6000-7000'	17	1.0	74.8	3,350	65.8	NA	0.1
	7000-8000'	24	1.7	87.1	14,028	152.7	NA	0.2
	8000-9000'	36	3.3	97.1	14,331	80.5	NA	1.9
	9000-10,000'	40	4.9	98.6	11,501	44.1	6.1 (1)	3.7
	10,000-11,000'	41	6.1	97.4	11,290	34.5	NA	4.2
	11,000-12,000'	42	7.1	97.9	6,150	16.2	NA	3.1
	> 12,000'	39	6.8	98.2	1,384	3.8	NA	1.9
Owens	5000-6000'	0	0.0	5.8	18	447.1	NA	0.0
	6000-7000'	5	0	15	1,724	359.6	NA	0.0
	7000-8000'	12	0.4	29.4	8,035	336.0	NA	0.1
	8000-9000'	22	1.0	43.8	10,612	190.7	NA	0.3
	9000-10,000'	35	2.6	75.2	21,707	154.5	2.1 (2)	0.7
	10,000-11,000'	39	4.2	91.0	37,782	168.8	1.6 (2)	1.2
	11,000-12,000'	42	5.7	90.1	40,982	135.6	NA	1.1
	> 12,000'	42	6.5	92.6	27,650	79.8	NA	0.7

* This is a comparison to the SNODAS (SNOw Data Assimilation System) nationwide product from the National Weather Service.

Location of Reports and Excel Format Tables

ftp://snowserver.colorado.edu/pub/Sierras

References and Additional Sources

Margulis, S. A., Cortés, G., Girotto, M., & Durand, M. (2016). A Landsat-Era Sierra Nevada Snow Reanalysis (1985–2015). *Journal of Hydrometeorology*, 17(4), 1203–1221, doi:/10.1175/JHM-D-15-0177.1

Molotch, N.P. (2009). Reconstructing snow water equivalent in the Rio Grande headwaters using remotely sensed snow cover data and a spatially distributed snowmelt model. *Hydrological Processes*, Vol. 23, doi: 10.1002/hyp.7206, 2009.

Molotch, N.P., and S.A. Margulis. (2008) Estimating the distribution of snow water equivalent using remotely sensed snow cover data and a spatially distributed snowmelt model: a multi-resolution, multi-sensor comparison. *Advances in Water Resources*, 31, 2008.

Molotch, N.P., and R.C. Bales. (2006). Comparison of ground-based and airborne snow-surface albedo parameterizations in an alpine watershed: impact on snowpack mass balance. *Water Resources Research*, VOL. 42, doi:10.1029/2005WR004522.

Molotch, N.P., and R.C. Bales. (2005). Scaling snow observations from the point to the grid-element: implications for observation network design. *Water Resources Research*, VOL. 41, doi: 10.1029/2005WR004229.

Molotch, N.P., T.H. Painter, R.C. Bales, and J. Dozier. (2004). Incorporating remotely sensed snow albedo into a spatially distributed snowmelt model. *Geophysical Research Letters*, VOL. 31, doi:10.1029/2003GL019063, 2004.

Painter, T.H., K. Rittger, C. McKenzie, P. Slaughter, R. E. Davis and J. Dozier. (2009) Retrieval of subpixel snow covered area, grain size, and albedo from MODIS. *Remote Sensing of the Environment*, 113: 868-879.

Rittger, K., M. S. Raleigh, J. Dozier, A. F. Hill, J. A. Lutz, and T. H. Painter. 2019. Canopy Adjustment and Improved Cloud Detection for Remotely Sensed Snow Cover Mapping. Water Resources Research 24 August 2019. doi:10.1029/2019WR024914.

Schneider D. and N.P. Molotch. (2016). Real-time estimation of snow water equivalent in the Upper Colorado River Basin using MODIS-based SWE reconstructions and SNOTEL data. *Water Resources Research*, 52(10): 7892-7910. DOI: 10.1002/2016WR019067.